

Effect of oil in multiphase flow on corrosion product film in large horizontal pipeline

Der Einfluß von Öl in Mehrphasenströmungen auf den Korrosionsproduktfilm in großen horizontalen Rohrleitungen

T. Hong*, M. Gopal and W.P. Jepson

The properties of corrosion product film formed on carbon steel pipelines under saltwater-oil-CO₂ multiphase flow are examined by AC impedance methods. Experiments are performed in a 101.6 cm I.D., 10 m long pipeline. Experimental results show that there are two reactions on the steel surface in saltwater-oil mixture. One is charge transfer, and the other is diffusion. By calculation of charge transfer resistance, R_t , and Warburg impedance coefficient, σ , it is found that, R_t in saltwater-oil mixture is much higher than that in saltwater. In saltwater-oil mixture, R_t and σ increase with immersion time. It is suggested that the porous corrosion film occurs on the surface of the steel, and that the film becomes compact when the immersion time increases. The longer the exposure time, the more compact the film, resulting in that the corrosion rate becomes lower.

Die Eigenschaften des Korrosionsproduktfilmes, der sich an Rohrleitungen aus unlegiertem Stahl in Salzwasser-Öl-CO₂-Mehrfasenströmungen bildet, wurde mit Hilfe von AC Impedanz-Methoden untersucht. Die Versuche erfolgten in einer 10 m langen Rohrleitung mit einem Innendurchmesser von 101,6 mm. Die experimentellen Ergebnisse zeigen, daß es auf der Stahloberfläche in der Salzwasser-Öl-Mischung zwei Reaktionen gibt: den Ladungstransport und die Diffusion. Durch Berechnung des Ladungstransportwiderstandes, R_t , und des Warburg-Impedanzkoeffizienten, σ , wurde festgestellt, daß R_t in der Salzwasser-Öl-Mischung wesentlich höher ist als im Salzwasser. In der Salzwasser-Öl-Mischung steigen R_t und σ mit der Tauchdauer an. Es wird angenommen, daß sich der auf der Stahloberfläche bildende poröse Korrosionsfilm mit zunehmender Tauchdauer verdichtet. Je länger die Auslagerungszeit umso kompakter wird der Film, was zu einer verminderten Korrosionsgeschwindigkeit führt.

1 Introduction

Corrosion in carbon steel pipelines under multiphase flow has long been a problem in the oil industry. A study to determine the corrosion behaviors under such multiphase flow conditions becomes very important. It has been known that the corrosion product layer plays an important role in corrosion process, especially localized corrosion. In order to recognize the mechanisms of corrosion in multiphase flow, examination of the corrosion product film formed on the surface of the pipeline is necessary.

It has been suggested by Crolet et al. [1–4] that the corrosion layers formed on steel in carbon dioxide environment are composed of an insoluble corrosion product, iron carbonate (FeCO₃), and/or undissolved component from the steel, namely cementite (Fe₃C). Many researchers have studied the corrosion film in brine solutions [5–7]. They found that iron carbonate is the main corrosion product in sweet corrosion of carbon steel. Their studies show that iron carbo-

nate scale formation (dissolution) depends on various parameters such as temperature, pH, CO₂ partial pressure, brine content, material composition, flow velocity and flow regimes.

Almost all of these studies, however, were carried out in single phase systems using deionized water, or brine solutions saturated with carbon dioxide. The effect of oil on corrosion film in multiphase flow has not been studied.

In this work, the corrosion film formed on the surface of carbon steel in pipelines under multiphase flow was studied by AC impedance measurement. The effect of addition of oil on the film was examined.

2 Experimental method

Experiments were carried out in 101.6 mm I.D., 15 m long acrylic pipeline. The schematic layout of the system is given in Fig. 1. The liquid is forced under gate E into the 101.6 mm I. D. The carbon dioxide gas is introduced into the system at port F. The gas/liquid mixture passes through the Plexiglas pipeline. For slug flow, a hydraulic jump is generated and moved into the test section G by controlling the gas flow at the inlet F using a needle valve in conjunction with a flow system. The slug flow in this work is characterized by dimensionless Froude number (Fr), which can be defined as the following formula 1 [8]

* T. Hong, M. Gopal and W.P. Jepson
NSF I/UCRC, Corrosion in Multiphase System Center, Institute for Corrosion and Multiphase Technology,
Ohio University, Athens, OH45701 (USA)

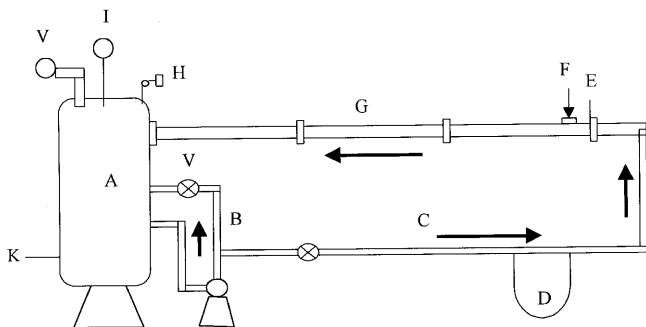


Fig. 1. A schematic of experiment system

Abb. 1. Schema des Versuchssystems

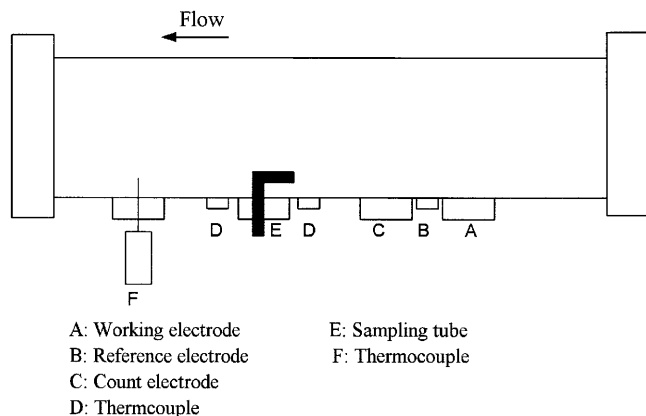


Fig. 2. A schematic of test section

Abb. 2. Schema des Testabschnittes

$$Fr = \frac{V_t - V_f}{(g \cdot h_{eff})^{1/2}} \tag{1}$$

Where

V_t = transnational velocity of the slug front (m/s).

V_f = average velocity of the liquid film (m/s).

g = the acceleration due to gravity (m/s^2).

h_{eff} = the effective height of the liquid film (m).

In this work, Froude number 6 (Fr 6) was used for slug flow.

The measurements were taken in the test section G as shown in Fig. 2. The material was a Type 1018 carbon steel rod of diameter of 9 mm. The chemical composition of the steel is given in Table 1. Before measurement, the test surface was polished with wet emery paper up to grade 600, and then cleaned by distilled water and acetone. The exposed electrode surface area was 0.71 cm^2 .

All potentials recorded in this work were referred to silver-silver chloride (Ag/AgCl), and the counter electrode was a polished stainless steel of diameter of 12.7 mm.

Test solutions were prepared by 100% ASTM substitute saltwater and 80% ASTM substitute saltwater and 20% LVT oil. The solutions were de-aerated by CO_2 gas for 4 h before experiments. The pH value in the solution is 5.4. All experiments were performed at 40 °C and 0.136 MPa.

AC impedance measurements were carried out after the working electrode had been immersed in the same solution for 20 min, and conducted at open circuit potentials. The AC impedance spectra in this work were generated by Gamry CMS300 corrosion monitoring system. A perturbation AC potential of amplitude 10 mV was applied over the frequency range from 0.01 Hz to 5 kHz.

3 Results and discussion

Fig. 3 shows the Nyquist impedance plots measured in saltwater under slug flow of Fr 6 at the open-circuit potential. In 100% saltwater, no diffusion tail can be observed from the impedance plots during four hours for immersion. This means that the electrode reaction is controlled by only charge transfer. This behavior can be interpreted according to a simple equivalent circuit model shown in Fig. 4a. Here, R_s is the solution resistance, R_t is the metal charge-transfer resistance, and C_{dl} is the double layer capacitance. R_s and R_t can be obtained by intersection of the high frequency portion of the semicircle with the resistive axis and the diameter of semicircle, respectively (see Fig. 5a).

Fig. 6 shows the Nyquist impedance plots measured in saltwater/oil/ CO_2 mixture under slug flow of Fr. 6 at the open-circuit potential. It is found that the diffusion tails appear and eventually become inclined at an angle of 45° to resistive axis. This means that there are two reaction processes on the surface: one is metal charge-transfer and the other is diffusion.

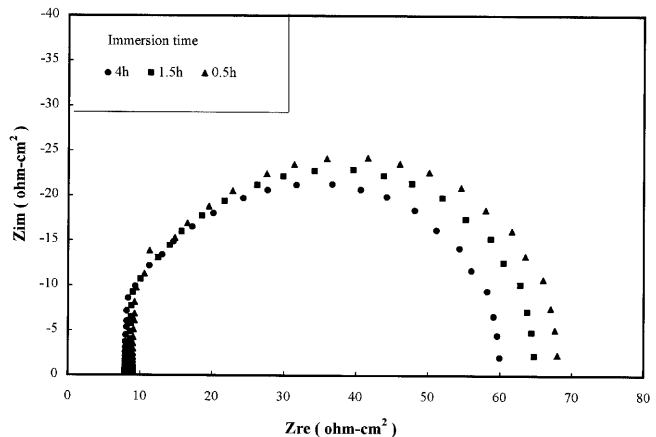


Fig. 3. The Nyquist impedance plots measured in 100% saltwater under Fr 6 slug flow at the open-circuit potential

Abb. 3. Nyquist-Impedanz-Diagramme, gemessen in 100% Salzwasser bei Fr-6-Strömung und freiem Korrosionspotential

Table 1. Chemical composition of type C-1018 carbon steel (wt%)

Tabelle 2. Chemische Zusammensetzung des unlegierten Stahles vom Typ C-1018 (Gew.-%)

C	Si	P	S	Mn	Al	Fe
0.21	0.38	0.09	0.05	0.05	0.01	Balance

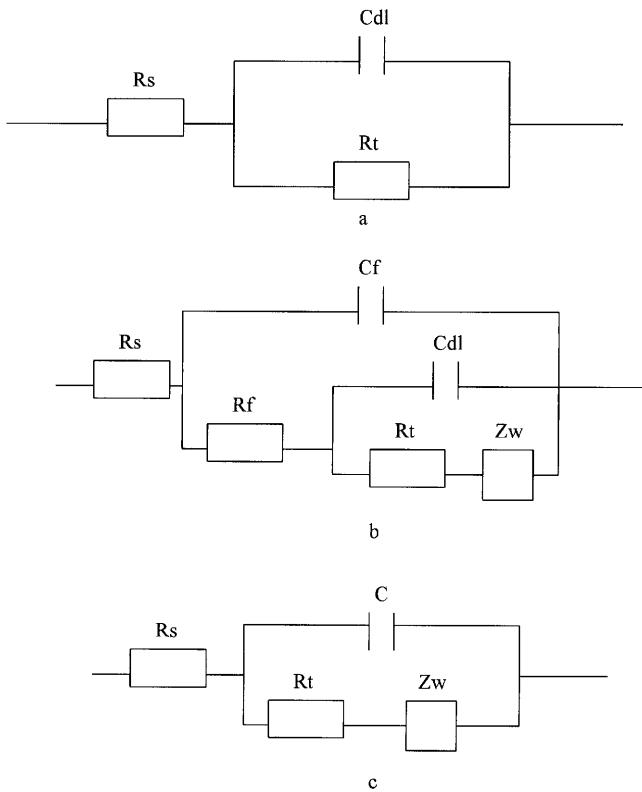


Fig. 4. Three models for the impedance data: (a) a model for metal equivalent circuit, (b) a standard model for filmed metal, and (c) a simple model for filmed metal

Abb. 4. Drei Modelle für die Impedanzdaten: (a) ein Modell für den Metalläquivalenzstromkreis, (b) ein Standardmodell für ein Metall mit Film und (c) ein einfaches Modell für ein Metall mit Film

Similar impedance behavior which consists of a diffusion tail at low frequencies has been reported for iron and iron-chromium by other researchers [9]. They suggested that the diffusion is due to appearance of the porous corrosion film formed on the surface. After experiments, by observation of the surfaces of the working electrode in saltwater and saltwater-oil mixture, it is found that no corrosion film forms on the surface in 100% saltwater solution. However, in saltwater-oil mixture, the corrosion deposits are very firmly held on the surface of the steel and are not easily removed by the sharp edge of a paper. Therefore, appearance of the diffusion on the electrode in 80% saltwater-20% oil indicates that the corrosion product film has been formed on the surface.

There are two methods to describe the EIS spectra for the filmed or rough electrodes. One is the finite transmission line model [10], and the other is the filmed equivalent circuit model [11]. In this work the filmed equivalent circuit model is used to describe the corrosion film covered on metal/solution interface.

The standard circuit model for filmed surface used extensively in the literature is shown in Fig. 4b [11]. Here R_f and C_f are the film resistance and capacitance, respectively, and Z_w is the Warburg impedance. Z_w can be presented as [12]

$$Z_w = \sigma \omega^{-1/2} (1 - j) \tag{2}$$

Where,

$$\sigma = \text{Warburg coefficient, } \text{Ohm}\cdot\text{cm}^2\cdot\text{s}^{-1/2};$$

$$\omega = 2 \pi f \text{ (rad s}^{-1}\text{)}.$$

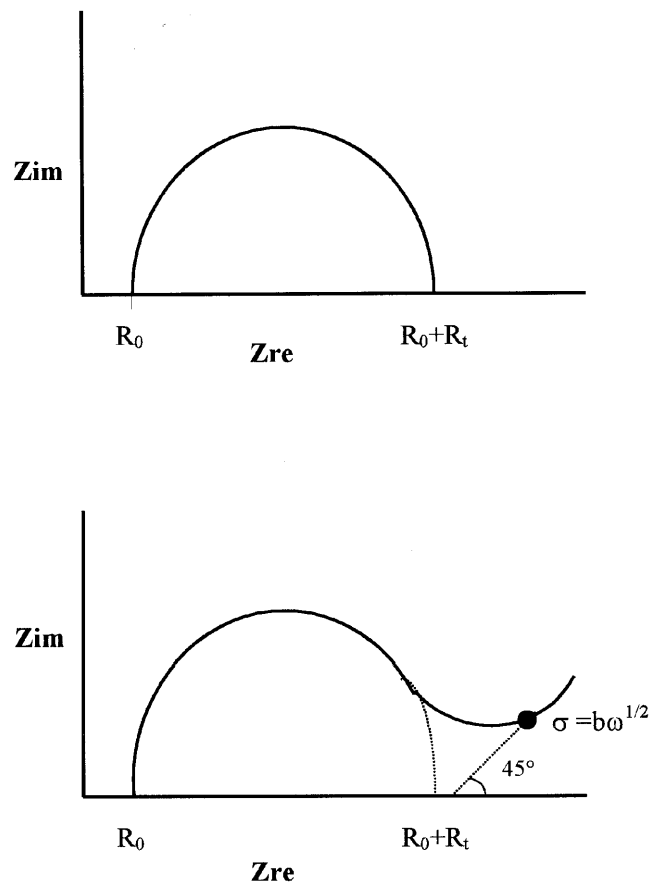


Fig. 5. Calculations of R_0 , R_t and σ using Nyquist plots

Abb. 5. Berechnungen von R_0 , R_t und σ mit Hilfe der Nyquist-Diagramme

The model as shown in Fig. 4b includes two parallel resistance and capacitance combinations and Warburg impedance, which are considered to contain corrosion film, metal substrate and diffusion information [11]. Two semicircles and a diffusion tail would be expected on the Nyquist plot. However, it is difficult to find two semicircles for C-1018 carbon

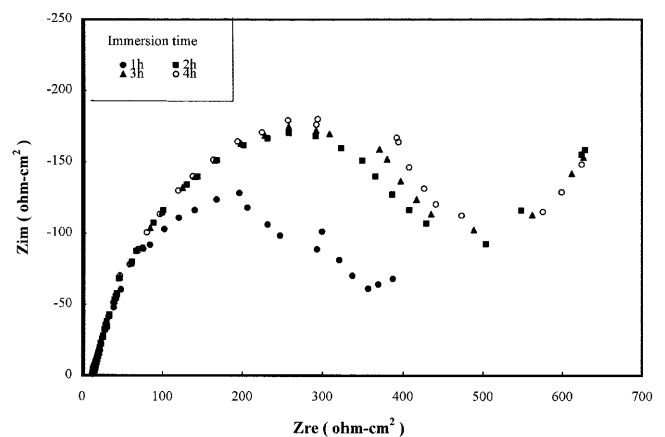


Fig. 6. The Nyquist impedance plots measured in 80% saltwater-20% oil mixture under Fr 6 slug flow at the open-circuit potential

Abb. 6. Nyquist-Impedanz-Diagramme, gemessen in einer 80% Salzwasser-20% Öl-Mischung bei Fr 6-Strömung und freiem Korrosionspotential

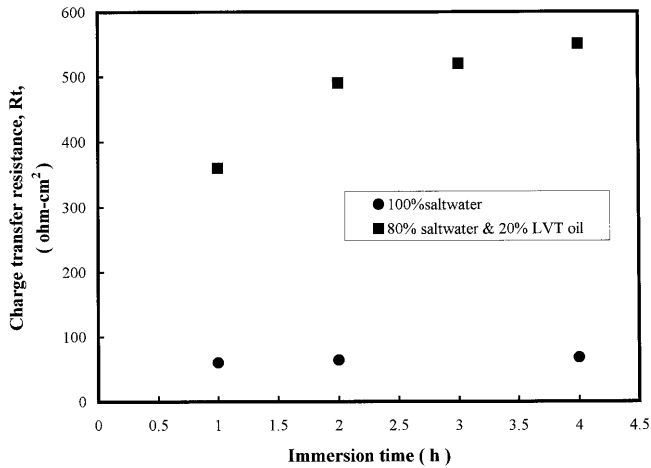


Fig. 7. The relationship between the immersion time and R_t in 100% saltwater and 80% saltwater-20% oil mixture

Abb. 7. Zusammenhang zwischen der Tauchdauer und R_t in 100% Salzwasser und in einer 80% Salzwasser-20% Öl-Mischung

steel exposed to the 80% saltwater-20% oil solution in Fig. 6. This could result from that the high rate of wall shear stress of the turbulent flow makes the corrosion film porous. The corrosion film resistance (R_p) might be much smaller than the charge transfer resistance (R_t). The semicircle representing the corrosion film merges with the charge transfer loop. In this case, the EIS spectra for the filmed surface as shown in Fig. 6 can be described by a simple equivalent circuit as shown in Fig. 4c.

The Warburg impedance coefficient σ can be obtained from Equation (3) by using the Nyquist impedance plots of Fig. 6 at low frequencies where the diffusion tails are inclined at the angles of 45° to the resistive axis as shown in Fig. 5b [12].

$$\sigma = b \omega^{1/2} \quad (3)$$

where

b = reactive component of impedance at which the diffusion tail begins to be inclined at an angle of 45° to the resistive axis, $\omega = 2\pi f$, i.e. f : a frequency at which the diffusion tail begins to be inclined at an angle of 45° to the resistive axis.

Fig. 7 summarizes the results of charge transfer resistance, R_t , measured in both solutions. It can be observed that R_t in 80% saltwater-20% oil mixture is much higher than that in 100% saltwater. This behavior can be explained by the following.

(1) In slug flow, because of high turbulence, the phases become well. The oil in this case touches the bottom of the pipe. This leads to a possible decrease in the corrosion rate.

(2) Because the corrosion product film is present on the surface of the steel in saltwater-oil mixture, the anodic dissolution is inhibited by the diffusion processes through the pores in the film, thus leading to low corrosion rate.

From Fig. 7 it can be also found that, in 100% saltwater, R_t is almost constant when the time increases. It can be considered that the corrosion rate is independent of time in 100% saltwater. In 80% saltwater-20% oil mixture as shown in Fig. 7, however, R_t increases with increase in immersion time. This behavior may be due to the occurrence of the corrosion film on the surface of the steel. Increase in R_t implies that the corrosion film is protective, and that the film becomes

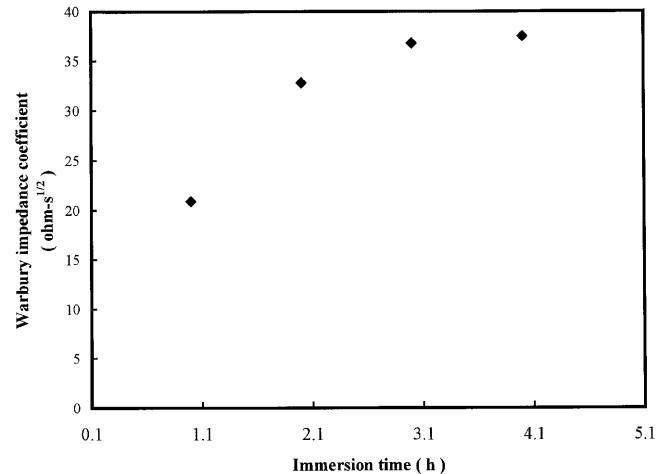


Fig. 8. The relationship between the immersion time and Warburg impedance coefficient in 80% saltwater-20% oil mixture under Fr 6 slug flow

Abb. 8. Zusammenhang zwischen der Tauchdauer und dem Warburg-Impedanzkoeffizienten in einer 80% Salzwasser-20% Öl-Mischung bei Fr 6-Strömung

compact gradually with increasing time. In this case, the corrosion probably is inhibited by the diffusion of ions in the film.

On the other hand, the Warburg impedance coefficient, σ , measured in 80% saltwater-20% oil mixture, increases with increase in immersion time as shown in Fig. 8. Since σ represents the resistance which comes from the diffusion process at the electrode, increase in σ indicates increasing the diffusion resistance. It has been suggested that the diffusion barriers on the electrode are provided by corrosion product film formed on the surface, and that the corrosion film formed on the steel surface is porous [9, 13–14]. Therefore, an increase in diffusion resistance on the surface implies improving the quality of the film, i.e. the porosity of the film decreases or the film thickness increases. In another word, the corrosion film becomes compact when the time increases. The longer the exposure time, the more compact the film, resulting in that the corrosion rate becomes lower. This is in a good agreement with the result obtained from charge transfer resistance measured in 80% saltwater-20% oil mixture as shown in Fig. 7.

4 Conclusions

The following conclusions are drawn from an AC impedance study of effect of oil on corrosion product film in multi-phase flow.

1. The metal charge-transfer resistance, R_t , in 80% saltwater 20% oil mixture is much higher than that in 100% saltwater. This might be due to that, in oil-water mixture, the oil touches the bottom of the pipe and the corrosion product film is present on the surface of the steel.
2. In 80% water-20% oil, the charge transfer resistance, R_t , and the Warburg impedance coefficient, σ , increase with increase in immersion time. These facts suggest that the corrosion film becomes compact with increase in time. An improvement of the film leads to a decrease in corrosion rate.

5 References

- [1] *J. Crolet*: In: Predicting CO₂ Corrosion in Oil and Gas Industry. European Federation of Corrosion Publications, No. 13 (London, U. K.: The institute of Materials, 1994).
- [2] *J. Crolet*: In: Predict CO₂ Corrosion in the Oil and Gas Industry, Working Party Report, Institute of Materials, London, 1994, p.1.
- [3] *J. Crolet, L. S. Olsen, W. Wilhelmsen*: CORROSION/95, Paper No. 188 (Houston, Tx: NACE, 1995).
- [4] *J. Crolet, L. S. Olsen, W. Wilhelmsen*: CORROSION/94, Paper No. 4 (Houston, Tx: NACE, 1994).
- [5] *C. De Waard, D. E. Milliams*: Corrosion 5 (1975) 636.
- [6] *C. De Waard, U. Lotz, D. E. Milliams*: Corrosion 11 (1991) 976.
- [7] *C. De Waard, U. Lotz*: CORROSION/93 Paper No. 50 (Houston Tx: NACE, 1993).
- [8] *X. Zhou, W. P. Jepson*: CORROSION/99, Paper No. 26 (Houston, Tx: NACE 1994).
- [9] *X. P. Guo, Y. Tomoe*: Corrosion 54 (1998) 931.
- [10] *J. R. Park, D. D. Macdonald*: Corros. Sci. 23 (1983) 295.
- [11] *L. Bousselmi, C. Fiaud, B. Tribollet, E. Triki*: Corros. Sci. 39 (1997) 1711.
- [12] *G. W. Walter*: Corros. Sci. 26 (1986) 81.
- [13] *J. H. Wang, F. I. Wei, H. C. Shih*: Corrosion 52 (1996) 600.
- [14] *T. R. Beck*: Electrochim, Acta 30 (1985) 725.

(Received: September 3, 1999)

W 3399